

Oleic Acid Inhibits Alveolar Fluid Reabsorption

A Role in Acute Respiratory Distress Syndrome?

István Vadász, Rory E. Morty, Markus G. Kohstall, Andrea Olschewski, Friedrich Grimminger, Werner Seeger, and Hossein A. Ghofrani

University of Giessen Lung Center, Justus Liebig University, Giessen, Germany

Levels of oleic acid (OA) are elevated in plasma and bronchoalveolar lavage fluids of patients with acute respiratory distress syndrome (ARDS). OA is also widely used to provoke edema, by unknown mechanisms, in experimental models of ARDS. We investigated the impact of intravascularly applied OA on epithelial lining fluid balance. OA (25 μ M) dramatically blocked active transepithelial $^{22}\text{Na}^+$ transport (by 92%) in an isolated, ventilated, and perfused rabbit lung model, provoking alveolar edema, assessed by increases in lung weight and epithelial lining fluid volume. OA did not alter epithelial permeability, measured by [^3H]mannitol and fluorescently labeled albumin flux, but did increase endothelial permeability, assessed by capillary filtration coefficient. In A549 cells, OA completely blocked amiloride-sensitive sodium currents measured by patch clamp, and also largely abrogated ouabain-sensitive Na^+, K^+ -ATPase-mediated $^{86}\text{Rb}^+$ uptake. Although OA did not alter epithelial sodium channel or Na^+, K^+ -ATPase surface expression, it covalently associated with both molecules and directly, dramatically, and dose-dependently inhibited the catalytic activity of purified Na^+, K^+ -ATPase. Therefore, OA impaired the two essential transepithelial active sodium transport mechanisms of the lung, and could thus promote alveolar edema formation and prevent edema resolution, thereby contributing to the development of ARDS.

Keywords: acute lung injury; alveolar epithelium; ENaC; Na^+, K^+ -ATPase

Acute respiratory distress syndrome (ARDS) has an incidence of up to 75 per 100,000 individuals (1) and exhibits mortality rates of more than 30% (2, 3). The hallmarks of ARDS include an increase in endothelial permeability (4) and loss of epithelial barrier function (5, 6), resulting in an accumulation of alveolar and interstitial edema fluid in the lung. The loss of alveolar-capillary barrier integrity impairs active fluid transport mechanisms in the lung, preventing reabsorption of edema fluid from the alveolar space, which is a key step in the resolution of ARDS. It is widely believed that edema fluid must be cleared for patients with ARDS to survive (7, 8).

The primary mechanism driving fluid clearance from the alveolus is the active transport of sodium from air spaces into the lung interstitium (9). This active vectorial sodium flux generates an osmotic gradient, which, in turn, promotes passive movement of water from the alveolar space into the interstitium (10). Sodium uptake by the alveolar epithelial cells occurs on the apical side, primarily through amiloride-sensitive ion channels, such as the epithelial sodium channel (ENaC) (11, 12), with subsequent active

pumping out from the basolateral surface by Na^+, K^+ -ATPase (13, 14). Thus, both ENaC (10) and the Na^+, K^+ -ATPase (15) are accredited with key roles in the resolution of pulmonary edema.

Perturbations to lipid metabolism and the activity of lipid-metabolizing enzymes, particularly acyltransferases and phospholipases, have been implicated in the pathogenesis of ARDS (16, 17). Serum samples from patients with ARDS have significantly elevated levels of oleic acid (OA), a C18:1 unsaturated ω -9 free fatty acid (16, 17). Similarly, at-risk patients who subsequently developed ARDS also exhibited higher serum OA levels (17). Patients with sepsis, of whom approximately 50% develop ARDS (2, 18), also exhibited a dramatic sixfold increase in plasma OA levels in comparison to plasma from healthy volunteers (19). Similarly, in an LPS-induced acute lung injury model, a 15-fold increase in free OA was observed in bronchoalveolar lavage (BAL) fluids from mice 8 hours after LPS application (20). The proportion of OA incorporated into surfactant phospholipids is also significantly elevated in patients with ARDS (21) and sepsis (22). Together, these observations have led investigators to propose OA as a prognostic factor for ARDS (17).

The observed elevation of OA levels in plasma and BAL samples from patients with ARDS is particularly interesting considering that OA-induced lung injury is an extensively used experimental model of ARDS (23). However, the precise mechanism by which OA induces lung edema formation remains to be clarified. OA has been described to cause an increase in pulmonary vascular permeability, within seconds of exposure (24), resulting in extravascular lung water accumulation (25). However, no study to date has addressed the influence that OA may have on transepithelial vectorial sodium transport and its implications for lung physiology and pathophysiology. This study examined the effect of OA on transepithelial sodium transport, and we consider these data in the context of a prognostic, and perhaps causal, role for OA in acute lung injury/ARDS.

Some of the results of these studies have been previously reported in the form of an oral address presented at the 100th International Congress of the American Thoracic Society, Orlando, Florida, May 21–26, 2004 (26).

METHODS

Lung Preparation and Handling

Lungs were isolated from healthy adult male rabbits (Charles River, Sulzfeld, Germany) that weighed 3.0 ± 0.5 kg, as previously described (27). Rabbits were anesthetized with ketamine (30–50 mg/kg intravenously) and xylazine (6–10 mg/kg intravenously), and heparin (1,000 U/kg) was applied as an anticoagulant. Animals were mechanically ventilated with room air with a Harvard cat/rabbit ventilator (Hugo Sachs Elektronik, March Hugstetten, Germany) through a tracheotomy. Catheters were inserted into the pulmonary artery and the left atrium, which were exposed by a midsternal thoracotomy, and perfusion was undertaken with Krebs-Henseleit buffer (120 mM NaCl, 4.3 mM KCl, 1.1 mM KH_2PO_4 , 25 mM NaHCO_3 , 2.4 mM CaCl_2 , 1.3 mM magnesium phosphate, 0.24% [mass/vol] glucose, and 5% [mass/vol] hydroxyethylamyllopectin) at a flow rate of 100 ml/minute with a left atrial pressure of 1.6 mm Hg. Lungs were freely suspended from a force transducer in a temperature-equilibrated housing chamber at 37°C (or at 4°C in the

(Received in original form July 22, 2004; accepted in final form November 8, 2004)

Supported by the Deutsche Forschungsgemeinschaft Schwerpunktprogramm 1028 and Sonderforschungsbereich 547 "Kardiopulmonales Gefäßsystem." I.V. is supported by a predoctoral fellowship from Altana Pharma. R.E.M. is a fellow of the Alexander von Humboldt Foundation.

Correspondence and requests for reprints should be addressed to Werner Seeger, M.D., University of Giessen Lung Center, Justus Liebig University, Klinikstrasse 36, D-35392 Giessen, Germany. E-mail: werner.seeger@innere.med.uni-giessen.de

Am J Respir Crit Care Med Vol 171, pp 469–479, 2005

Originally Published in Press as DOI: 10.1164/rccm.200407-9540C on November 12, 2004

Internet address: www.atsjournals.org

case of low-temperature experiments) and ventilated with room air supplemented with 4.5% CO₂ to maintain pH of the recirculating buffer between 7.35 and 7.37. Peak inspiratory pressure was set to 7.5 mm Hg. A frequency of 30 breaths/minute and an inspiratory/expiratory ratio of 1:1 with a positive end-expiratory pressure of 2 mm Hg were applied to prevent atelectasis and to maintain constant minute volume during the experiment. Perfusion pressure, ventilation pressure, and the weight of the isolated organ were continuously monitored online.

Treatment of Lungs

Lungs were routinely maintained for 30 minutes to establish baseline conditions, after which OA (25- μ M final concentration, dissolved in a 1:1 mixture of H₂O to ethanol as vehicle) or vehicle alone was applied to the perfusate. Lungs were allowed to reestablish steady-state baseline conditions for 30 minutes, after which they were nebulized with amiloride in 2.5% (vol/vol) dimethyl sulfoxide in physiologic saline, yielding a concentration of 10 μ M in the epithelial lining fluid (ELF), or with physiologic saline (in the case of a sham nebulization). In some experiments, both OA and amiloride were applied sequentially in the same experiment, as described previously. Experiments were conducted either at 37°C or at 4°C. After a 30-minute reequilibration period, radioactive tracers were applied by ultrasonic nebulization of a mixture of ²²NaCl (1 μ Ci/ml) and [³H]mannitol (6 μ Ci/ml) in physiologic saline, over 10 minutes, with an Optineb ultrasonic nebulizer (Nebu-Tec, Elsenfeld, Germany), connected directly to the inspiration loop of the ventilator. More than 90% of the aerosol that reached the lung was deposited into the alveolar space, leading to a tracer deposition of approximately 1.2 μ Ci ²²Na⁺ and approximately 7.2 μ Ci [³H]mannitol. The elimination of ²²Na⁺ from the lung was monitored by γ -detectors (Target System Electronic, Solingen, Germany) placed around the lung and perfusate reservoirs for 90 minutes after nebulization. Transit of the [³H]mannitol tracer was followed by discontinuous perfusate sampling (at 5, 10, 15, 20, 30, 50, and 90 minutes after nebulization) and was quantified by scintillation counting in a Canberra Packard β -counter (Packard, Dreieich, Germany). Tracer-clearance curves were referenced to a 100% starting point at the end of nebulization. As an alternative to the radioactive tracers ²²Na⁺ and [³H]mannitol, a second, independent measurement of epithelial permeability was fluorescein isothiocyanate (FITC)-labeled albumin flux from the perfusate into the alveolar space. The FITC-albumin was added to the perfusate (at a final concentration of 0.16 mg/ml) 30 minutes after sham treatment or OA or H₂O₂ (300 μ M; positive control) application. The FITC-albumin concentrations were determined from BAL fluids (200 μ l) in a Fusion (Packard) microplate spectrofluorimeter at an emission wavelength of 480 nm and an excitation wavelength of 520 nm, as described elsewhere (28). The experimental protocol was identical to that described previously for the radioactive ²²Na⁺ and [³H]mannitol transit kinetics. ELF volume was determined from sodium concentrations of BAL fluids as described previously (29).

Assessment of Endothelial Permeability

Capillary filtration coefficients (K_{fc}) were used to assess changes in endothelial permeability. Coefficients were determined gravimetrically from the slope of the lung weight-gain curve induced by a 7.5-mm Hg step elevation of the venous pressure for 10 minutes, as described previously (30, 31). These experiments were performed separately from the studies addressing ²²Na⁺ and [³H]mannitol fluxes.

Electrophysiology

To investigate changes in macroscopic current of epithelial cells caused by OA and amiloride, the conventional whole-cell patch-clamp technique (32) was used. Human lung epithelial A549 cells (American Type Culture Collection; Manassas, VA) contain amiloride-sensitive sodium channels with biophysical properties similar to those of type II alveolar epithelial cells (33). We therefore used A549 cells as a model lung epithelial cell in our studies. Cells were plated on 16-mm-diameter glass cover slips and mounted in a flow-through chamber on the stage of an inverted microscope (Axiovert 135; Zeiss, Jena, Germany) and perfused (2–3 ml/minute) with 145 mM NaCl, 2.7 mM KCl, 1.8 mM CaCl₂, 2 mM MgCl₂, 5.5 mM glucose, and 10 mM *N*-2-hydroxyethylpiperazine-*N'*-ethane sulfonic acid, pH 7.4, at room temperature. Pipettes pulled from borosilicate glass tubes (GC 150; Clark Electromedical Instruments,

Pangbourne, UK) were fire-polished to give a final resistance of 3 to 5 M Ω , and back-filled with 135 mM potassium methylsulfonic acid, 10 mM KCl, 6 mM NaCl, 1 mM Mg₂ATP, 2 mM Na₂ATP, 5.5 mM glucose, 10 mM *N*-2-hydroxyethylpiperazine-*N'*-ethane sulfonic acid, 0.5 mM ethyleneglycol-*bis*-(β -aminoethyl ether)-*N,N'*-tetraacetic acid, pH 7.4. The effective corner frequency of the low-pass filter was 5 kHz. The frequency of digitization was twice that of the filter frequency. Offset potentials were nulled directly before formation of a seal. Series resistance and membrane capacitance were compensated before the onset of recordings with an Axopatch 200B amplifier (Axon Instruments, Foster City, CA). Experiments were performed at room temperature (22°C) or in selected cases at 8°C. Inward and outward currents across the cell membrane were elicited by using a step-pulse protocol from -100 to +100 mV in 10-mV increments for 500 milliseconds from a holding potential of -40 mV. Current-voltage relationships were constructed by averaging the current values between 100 and 500 milliseconds from the start and plotted using Origin software (Microcal Software, Northampton, MA). These measurements were repeated with perfusate containing OA or amiloride. The drug-sensitive currents were calculated by subtracting the current remaining after exposure to OA or OA and amiloride from the corresponding control (no drug) values (33).

Ouabain-sensitive Rb Uptake Assay

Ouabain-sensitive uptake of the K⁺-mimic ⁸⁶Rb⁺ into A549 cells was used to estimate potassium transport mediated by Na⁺,K⁺-ATPase, essentially as described by Ridge and colleagues (34). Cells, plated in six-well plates, were incubated in Dulbecco's modified Eagle medium:F12 (1:1), supplemented with 10% (vol/vol) fetal calf serum in the absence or presence of ouabain (1.67 mM), OA (1 nM–250 μ M), or ethanol (0.17% [vol/vol]), which served as a vehicle control, for 5 minutes at 37°C in a Heidolph UniMax 1010 incubator (Heidolph Instruments, Schwabach, Germany) with gentle (100-rpm) gyration. Media were aspirated off and replaced with identical fresh medium containing 1 μ Ci/ml ⁸⁶Rb⁺, and plates were incubated for a further 5 minutes (37°C, 100 rpm). Rb uptake was terminated by aspiration of the medium and the addition of 10 mM ice-cold Tris-Cl and 150 mM MgCl₂, pH 7.4. Wells were washed extensively with 10 mM Tris-Cl and 150 mM MgCl₂ (3 \times 5 ml), and plates were air-dried overnight. Cells were solubilized in 0.2% (m/v) sodium dodecyl sulfate, and ⁸⁶Rb⁺ in the cell extracts was quantified by liquid scintillation counting in a Canberra Packard β -counter (Packard). Protein was quantified with the BioRad D_c protein assay reagent (BioRad, Munich, Germany), which is based on the method of Bradford (35), adapted for samples containing detergents.

Immunoprecipitation, Cell-Surface Biotinylation, and Acylation Studies

Protein extracts were prepared from A549 cells by scraping in 1 ml of cell-lysis buffer (50 mM Tris-Cl, pH 7.4, containing 100 mM NaCl, 50 mM NaF, 5 mM β -glycerophosphate, 2 mM ethylenediaminetetraacetic acid, 2 mM ethyleneglycol-*bis*-(β -aminoethyl ether)-*N,N'*-tetraacetic acid, 1 mM sodium orthovanadate, 0.1% Triton X-100, and 25 \times protease inhibitor cocktail [Roche, Mannheim, Germany]) per 10-cm-diameter tissue culture dish. Extracts (1 ml) were briefly vortexed (2 \times 5 seconds). Extracts were incubated with protein G-agarose beads and 5 μ g of the relevant antibody (goat anti-Na⁺,K⁺-ATPase α subunit [Santa Cruz, Santa Cruz, CA] or rabbit anti-ENaC β subunit [Calbiochem, San Diego, CA]) by end-over-end mixing (16 hours, 4°C). Beads were washed (3 \times 1 ml, 4°C) and boiled in sample buffer (100 μ l); the supernatants were resolved by Tris-Tricine sodium dodecyl sulfate polyacrylamide gel electrophoresis (SDS-PAGE) on a 10% polyacrylamide gel (36), transferred to an Immobilon-P membrane (Amersham, Buckinghamshire, UK), and probed for Na⁺,K⁺-ATPase (with mouse anti-Na⁺,K⁺-ATPase α subunit [Sigma, Disenhofen, Germany]) or ENaC (with goat anti-ENaC β subunit [Santa Cruz]). Immune complexes were detected with peroxidase-conjugated secondary antibodies and visualized by enhanced chemiluminescence (Amersham).

Biotinylation of cell-surface proteins of A549 cells was undertaken as described in Dada and coworkers (37). Cell monolayers (80–90% confluent in 10-cm-diameter tissue culture dishes) were washed with phosphate-buffered saline and maintained on ice. Cells were labeled (4°C, 1 hour) with 1 mg/ml EZ-link *N*-hydroxysuccinamide-SS-biotin (Pierce, Rockford, IL) in PBS (1 ml), rinsed six times with 50 mM

glycine in phosphate-buffered saline to quench unreacted activated biotin, and then lysed in cell-lysis buffer (described previously). Cell extracts were incubated with end-over-end shaking (16 hours, 4°C) with streptavidin-agarose beads (Pierce). Beads were washed (4 × 1 ml, 4°C) and boiled in sample buffer (100 μl), and the supernatants were resolved, transferred to an Immobilon-P membrane (Amersham), and probed for Na⁺,K⁺-ATPase and ENaC as described previously.

To investigate whether OA covalently associated with either Na⁺,K⁺-ATPase or ENaC, cell monolayers were incubated with (9,10[*n*]-³H)OA (50 μCi/ml; Amersham) for 1 hour. Monolayers were washed (10 × 10 ml) with phosphate-buffered saline, lysed, and immunoprecipitated as described previously. Immunoprecipitates were split between two gels, one of which was probed by immunoblotting for Na⁺,K⁺-ATPase or ENaC, whereas the other was subjected to autoradiography for 3 weeks at -70°C.

Na⁺,K⁺-ATPase Activity Assay

The Na⁺,K⁺-ATPase-catalyzed hydrolysis of ATP was determined essentially as previously described (38). The direct effect of OA on catalytic activity was determined by preincubating the catalytic α subunit of Na⁺,K⁺-ATPase (5 mU; Sigma) in assay buffer (33.3 mM imidazole, 167 mM NaCl, 50 mM KCl, pH 7.2; 267 μl) with varying concentrations of OA (100 nM–100 μM) for 5 minutes at 37°C. Substrate (25 mM ATP, 50 mM MgCl₂, pH 7.2; 67 μl) was added, and the reactions incubated at 37°C for a further 20 minutes, after which stop solution (50 mg/ml FeSO₄ in 3% [vol/vol] H₂SO₄, 1% [m/v] ammonium molybdate; 1.5 ml) was added and the concentration of the phosphomolybdate complexes determined at 700 nm in a BioRad SmartSpec 3000 (BioRad). The inclusion of ouabain (1.67 mM) served as a negative control.

Statistical Treatment of Data

Numeric values are given as the mean ± SD. Intergroup differences were assessed by a factorial analysis of variance with *post hoc* analysis with Fisher's least significant difference test, where *p* values less than 0.05 were considered significant.

RESULTS

Oleic Acid Blocks Transepithelial Active Sodium Transport in Intact Lungs

At 37°C, approximately 62% of the ²²Na⁺ was cleared from lungs by the end of the experiment (Figure 1). This clearance was

mediated by both active and passive transport processes. When the lung was cooled to 4°C, only 48% of the ²²Na⁺ nebulized into the lung was cleared over the same time course. Sodium clearance at 4°C is attributable exclusively to passive transport processes, because active processes are shut down at this temperature (39). OA (25-μM perfusate concentration) and amiloride (an ENaC inhibitor; 10-μM ELF concentration) applied at 37°C impaired transepithelial sodium flux, reducing the clearance of the ²²Na⁺ tracer from a lung maintained at 37°C to 50 and 46%, respectively. These data indicate that OA significantly impairs transepithelial sodium flux.

Passive epithelial paracellular permeability, measured by [³H]mannitol clearance from the lung, was not significantly affected by low temperature, OA, or amiloride, when compared with control lungs at 37°C (Figure 2, *solid bars*). Thus, we reasoned that clearance of the fraction of ²²Na⁺ from the lungs at 37°C that was not cleared at 4°C was attributable to active processes, because passive processes were unaffected under all experimental conditions used. This “active transport” fraction is represented in Figure 1 by the difference between the area above the curve for the warm (37°C) and cold (4°C) control lungs. The effects of OA and amiloride specifically on active ²²Na⁺ clearance from the lung could thus be quantified (Figure 2, *open bars*).

Transepithelial active ²²Na⁺ transport was significantly (*p* < 0.001) reduced by 92 ± 3% when OA (25-μM final concentration) was applied to the perfusate (Figure 2). Similarly, without exhibiting any effect on the passive [³H]mannitol flux, amiloride (10 μM in the ELF) significantly (*p* < 0.001) reduced active sodium transport by 58 ± 6% compared with control (untreated) lungs. This finding is consistent with reports that approximately 50% of the sodium transport channels in mammalian lungs are amiloride-sensitive (10, 40). There was no additional inhibition of active sodium transport when OA was applied with amiloride (Figure 2), suggesting that OA blocked amiloride-sensitive sodium channels in addition to other sodium transport processes (one candidate being the Na⁺,K⁺-ATPase). To strengthen our

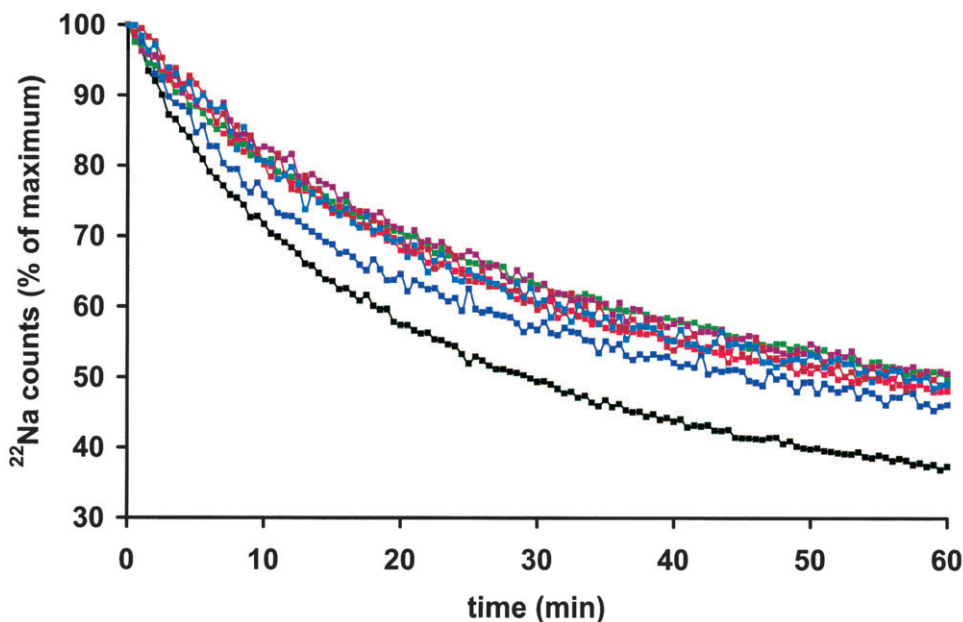


Figure 1. ²²Na⁺ clearance from isolated, ventilated, and perfused rabbit lungs is impeded by oleic acid (OA), amiloride, and low temperature. Lungs were maintained either at 37°C (*black*) or 4°C (*green*) and sham-nebulized with physiologic saline 30 minutes after establishing a steady-state equilibrium. After a further 30 minutes, ²²Na⁺ tracer was nebulized to the lung, and elimination of this tracer from the lung was monitored over 60 minutes. In additional experiments, OA (25-μM final concentration) was applied to the perfusate of lungs maintained at 37°C (*red*) or at 4°C (*light blue*) after establishing a steady-state equilibrium. Alternatively, instead of sham-nebulization, amiloride (10-μM final concentration in the epithelial lining fluid) was nebulized to lungs maintained at 37°C (*blue*) or at 4°C (*brown*). In a separate set of experiments, both OA and amiloride were applied together sequentially (*magenta*). Counts were set at 100% immediately

after nebulization of ²²Na⁺ tracer into the lungs. Each data point represents the mean of six independent experiments. For clarity, SDs (which were always < 2%, with the exception of control lungs and amiloride-treated lungs at 37°C, which were 4 and 3%, respectively) have been omitted. However, they are incorporated into the analyses of these data in Figure 2.

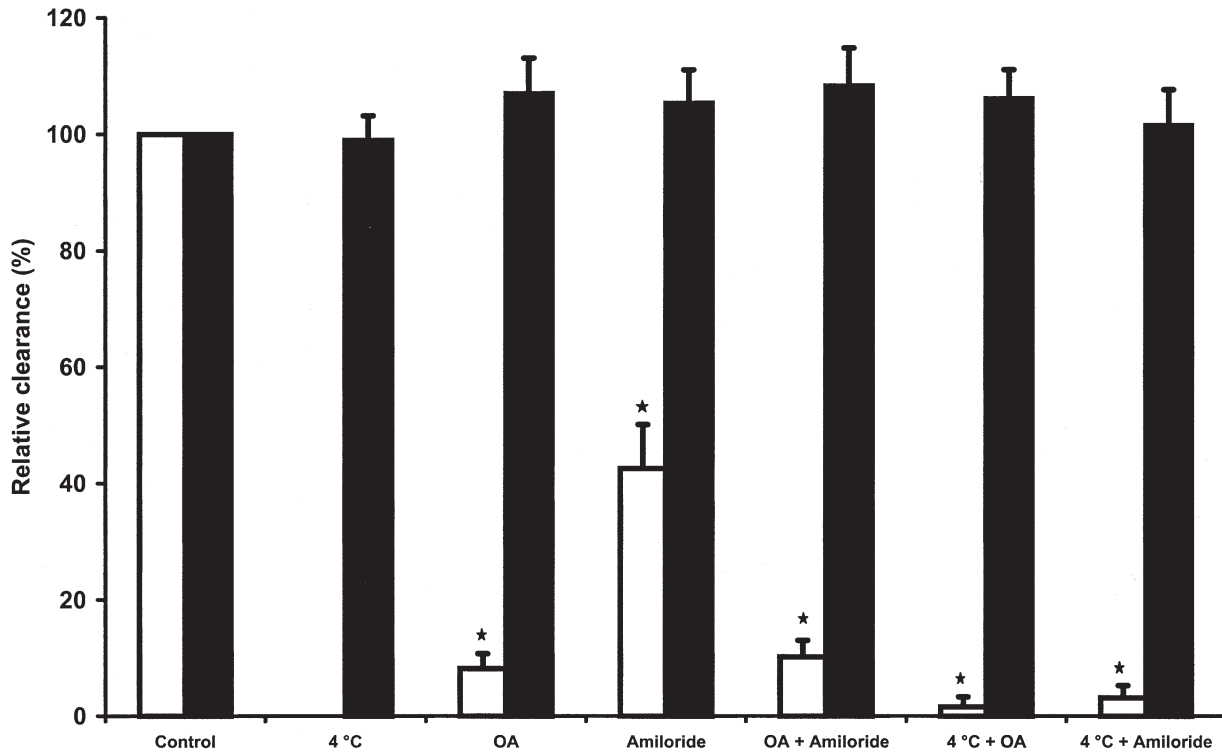


Figure 2. OA completely blocks active sodium transport without affecting passive paracellular epithelial permeability of intact lungs. Active $^{22}\text{Na}^+$ transport (open bars) was quantified from the data in Figure 1 as described in METHODS. The active $^{22}\text{Na}^+$ transport in untreated lungs maintained at 37°C was set at 100%, with the active $^{22}\text{Na}^+$ transport in treated lungs expressed relative to this control value. Passive ^3H mannitol flux (solid bars) was monitored by scintillation counting of perfusate samples taken at timed intervals after nebulization of the ^3H mannitol tracer to the lungs, as described in METHODS. The passive ^3H mannitol flux in untreated lungs maintained at 37°C was set at 100%, and mannitol flux in treated lungs was expressed relative to this control value. No active transport occurs at 4°C , hence there is no value for this parameter in the figure. Bars represent the mean \pm SD ($n = 6$ for all groups except OA + amiloride, $4^\circ\text{C} + \text{OA}$, and $4^\circ\text{C} + \text{amiloride}$, all at $n = 4$); * $p < 0.001$.

hypothesis, we applied OA or amiloride to lungs maintained at 4°C . Neither OA nor amiloride had any effect on transepithelial sodium flux at 4°C (Figure 2). These data suggest that passive transport processes were not altered after administration of OA, whereas active transport processes were completely blocked.

Because ^3H mannitol is a marker for paracellular epithelial permeability to small solutes, we further investigated any effect that OA may have on large solute permeability, which would result from any gross epithelial injury. We therefore monitored passage of FITC-albumin from the vascular space (the perfusate) to the alveolar space (represented by BAL fluids). In control, sham-treated lungs, BAL fluids yielded fluorescence values of 67 ± 14 arbitrary fluorescence units/ml ELF, whereas in lungs treated with $25 \mu\text{M}$ OA, the average fluorescence was 71 ± 20 arbitrary fluorescence units/ml ELF, which was comparable to untreated, control lungs. In contrast, after application of $300 \mu\text{M}$ H_2O_2 in the perfusate, which would generate gross epithelial damage, the BAL fluid fluorescence increased tenfold to 640 ± 170 arbitrary fluorescence units/ml ELF. From these data, we conclude that OA did not cause gross epithelial damage at the concentrations and route of administration used in our studies.

In control lungs that were not nebulized at any point, no apparent change in lung weight was observed over the course of the experiment (results not shown). However, control lungs maintained at 37°C and sham nebulized with physiologic saline exhibited a nonsignificant change in lung weight (0.12 ± 0.1 -g loss; Figure 3A) over the time course of the experiment. Thus, there was no progressive edema formation in the control lungs.

There was a *transient* weight gain immediately after each nebulization step, because each nebulization consistently deposited approximately 1 ml (SD $< 8\%$) of fluid per nebulization (i.e., ~ 2 ml in total/experiment) was deposited into the lung. But this excess fluid was fully cleared from the control lungs maintained at 37°C by the end of the experiment. However, in the case of lungs maintained at 4°C , where active transport was blocked, there was a net weight gain of 1.5 ± 0.3 g (corresponding to 1.5 ml of excess fluid). In line with our $^{22}\text{Na}^+$ transport data, OA (applied at $25 \mu\text{M}$ in the perfusate) caused a weight gain of 1.8 ± 0.4 g, and amiloride induced a total weight gain of 1.0 ± 0.2 g. Thus, when active transport processes are blocked (by either low temperature, OA, amiloride, or combinations thereof), the fluid that was nebulized into the lungs could not be cleared. It is critical to observe that the net weight gain of the treated lung is attributable to fluid that has been nebulized into the lung but cannot subsequently be cleared.

These observations are corroborated by estimation of the ELF volume under these experimental conditions. In control lungs maintained at 37°C , the ELF volume was kept constant at approximately 2.38 ± 0.24 ml (Figure 3B). When lungs were maintained at 4°C , the ELF volume increased to 4.39 ± 0.22 ml, indicating an average increase of 2.01 ml in ELF volume. Similarly, treatment with OA and amiloride increased the ELF volume by 2.28 and 0.92 ml, respectively. Our data are supported by similar experiments performed in rats, where amiloride caused a comparable decrease in alveolar fluid clearance (41). Similarly, when OA and amiloride were applied together, or when OA or

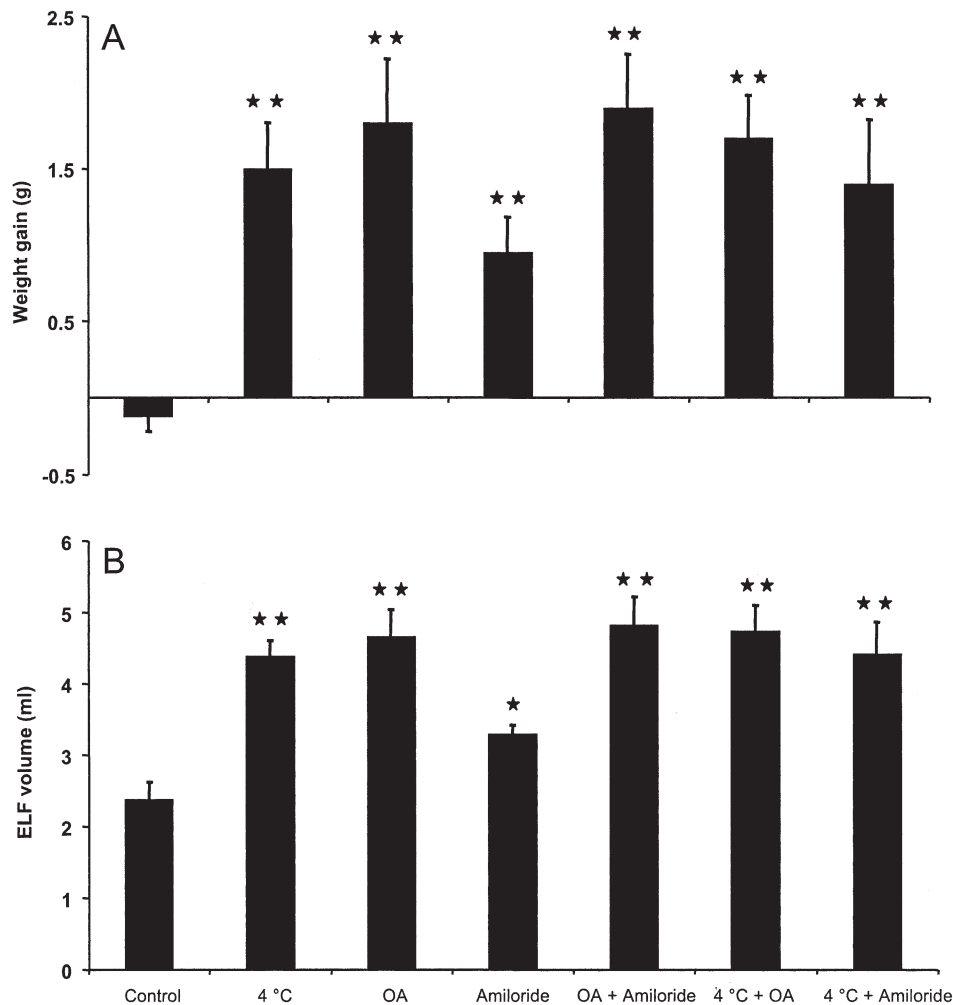


Figure 3. OA provokes edema formation in intact lungs. Fluid accumulation in the isolated, ventilated, and perfused rabbit lungs was estimated from the net lung weight gain, which was continuously monitored online throughout the experiment (A) and by determination of the epithelial lining fluid (ELF) volume from bronchoalveolar lavage fluids (B), as described in METHODS. Lungs were either maintained at 37°C or at 4°C to block active transport. In additional experiments, OA (25- μ M final concentration) was applied to the perfusate, or amiloride was applied to the alveolar space by nebulization (10- μ M final ELF concentration), or both agents were applied sequentially in the same experiment, as described in METHODS. Data represent the mean \pm SD ($n = 6$ for all groups, except OA + amiloride, 4°C + OA, and 4°C + amiloride, all at $n = 4$); * $p < 0.01$; ** $p < 0.001$.

amiloride were applied separately to lungs maintained at 4°C, an ELF volume increase of approximately 2.2 ml was again observed. The increase in the ELF volume correlated significantly ($p < 0.01$) with the increases in lung weight, suggesting that the edema we observed was primarily attributable to fluid accumulation in the alveolar space.

Oleic Acid Increases Endothelial Permeability in Intact Lungs

There was no change in the endothelial permeability of the isolated, perfused, and ventilated control rabbit lungs maintained at 37°C, as indicated by essentially unchanged K_{fc} values determined at 30, 70, and 110 minutes after the lungs reached steady-state equilibrium (Figures 4A and 4B). Similarly, lungs maintained at 4°C exhibited no perturbations to endothelial permeability over the 120-minute time course (Figure 4A), which was also observed with amiloride. In contrast to these data, OA caused a significant ($p < 0.05$) 1.8-fold increase in the endothelial permeability, as assessed by K_{fc} after exposure to 25 μ M OA (the same concentration used in radioactive tracer elimination studies; Figures 4A and 4C).

Oleic Acid Blocks Whole-Cell Current in A549 Cells

In the whole-cell mode, A549 cells exhibited inward rectifying currents carried by sodium (33). The inclusion of OA (10 μ M) in the perfusion fluid significantly ($p < 0.01$) reduced the inward sodium current and shifted the reversal potential to +41 mV. Representative whole-cell currents that were recorded during

control and after exposure to 10 μ M OA are shown in Figure 5A. Control recordings were made in the presence of 10 μ M ethanol (vehicle control, the same concentration as was used in the isolated, ventilated, and perfused rabbit lung model) to exclude nonspecific effects. The effect of OA on the outward potassium current was not significant. The averaged current-voltage relationship of OA-sensitive and OA-plus-amiloride-sensitive current is shown in Figure 5B.

Extracellular application of OA (10 μ M) inhibited whole-cell current to $55 \pm 11\%$ at -100 mV (Figure 5C; $n = 6$). To investigate the effect of amiloride on the remaining current, the whole-cell current was recorded in cells treated simultaneously with amiloride and OA (each at 10 μ M), in cells treated with amiloride (10 μ M) after a 5-minute pretreatment with OA (10 μ M), and in cells treated with OA (10 μ M) after a 5-minute pretreatment with amiloride (10 μ M). In all cases, the results were identical: amiloride had no appreciable effect on the OA-sensitive current, suggesting that OA blocks amiloride-sensitive channels (Figures 5B and 5C). The inhibition caused by OA was not reversible, because attempts to wash out the OA with perfusion fluid over a 30-minute time period did not restore a control response. It was unlikely that OA had any deleterious effect on the A549 cells, because there was no change in the leak current after OA administration.

Parallel recordings made at 8°C (to corroborate our data obtained in isolated, ventilated, and perfused rabbit lungs at low temperature) are shown in Figures 5B and 5C. Low temperature

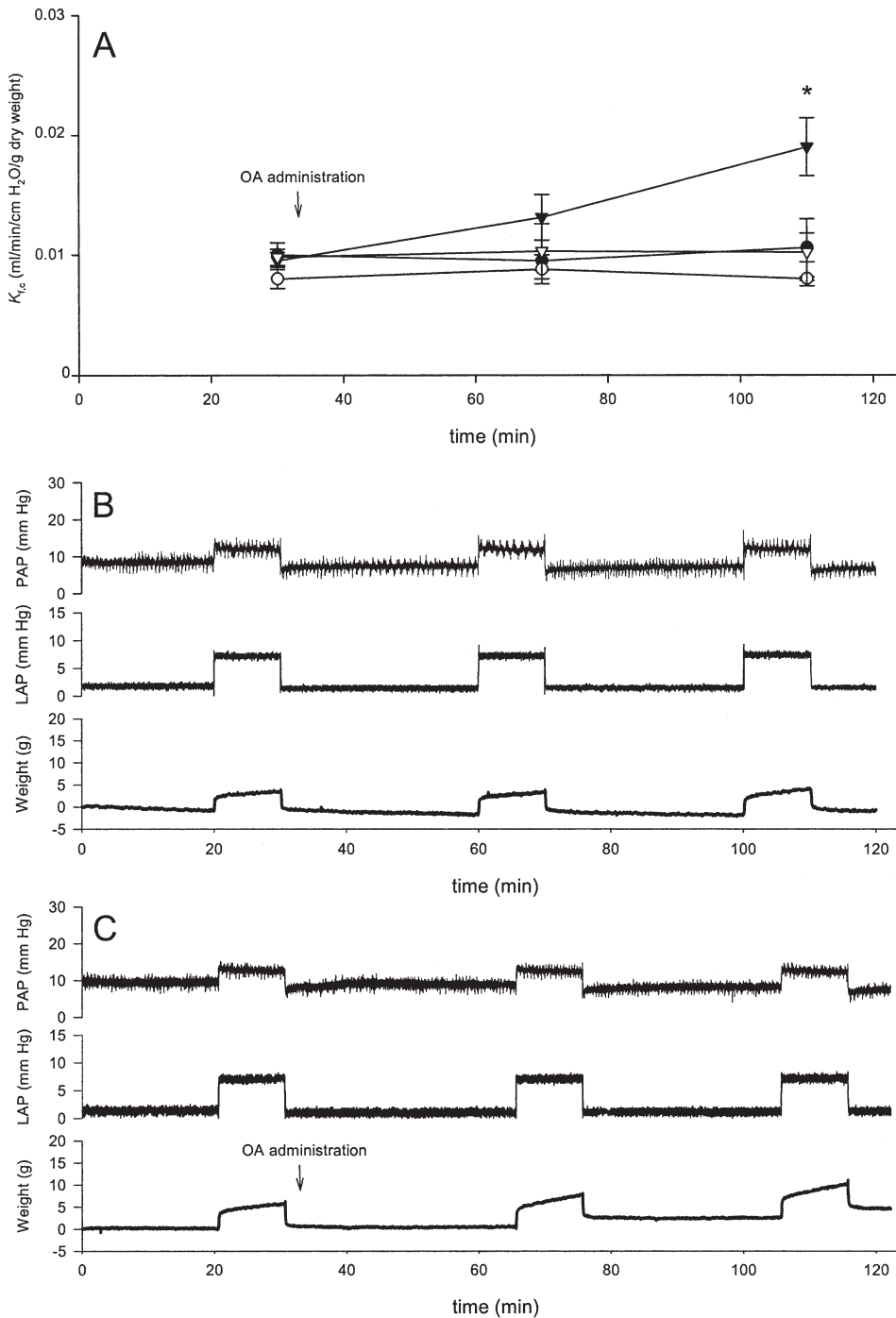


Figure 4. OA increases endothelial permeability of intact lungs. (A) Endothelial permeability was assessed from capillary filtration coefficients (K_{fc}) determined for lungs maintained at 37°C (solid circles) or at 4°C (open circles). Coefficients were also determined after administration of 10 μ M (final concentration) amiloride (inverted open triangles) to the ELF, or 25 μ M (final concentration) OA (inverted solid triangles) to the perfusate. Data represent the mean \pm SD ($n = 4$ for each group); * $p < 0.05$. Original representative recordings of pulmonary arterial pressure (PAP), left atrial pressure (LAP), and lung weight for a control lung (B) and an OA-treated lung (C) at 37°C are indicated.

resulted in a fourfold decrease (down to $23 \pm 8\%$) in whole-cell current, compared with whole-cell current at 22°C at -100 mV. OA, and amiloride applied either separately or together at 8°C did not significantly alter the whole-cell current when compared with untreated cells maintained at 8°C. Thus, the function of amiloride-sensitive sodium channels that were impaired by OA was also impaired by low temperature.

Oleic Acid Impairs Na^+ , K^+ -ATPase Function in A549 Cells

The activity of Na^+ , K^+ -ATPase in A549 cells was estimated from ouabain-sensitive $^{86}\text{Rb}^+$ uptake. OA (100 nM–250 μ M) caused a significant ($p < 0.001$), dose-dependent decrease in Na^+ , K^+ -ATPase activity, abrogating 83% of the activity at 250 μ M

OA (Figure 6), whereas vehicle alone (0.17% [vol/vol] ethanol) had no effect on $^{86}\text{Rb}^+$ uptake. At concentrations of 10 to 100 μ M OA, Na^+ , K^+ -ATPase function in A549 cells was still inhibited by 60 to 65%. The OA concentration that was applied in the isolated, ventilated, and perfused rabbit lungs (25 μ M) fell within this range.

Oleic Acid Does Not Alter Cell-Surface Expression of Na^+ , K^+ -ATPase or ENaC, but Does Associate with Both Molecules

No significant change in the cell-surface expression of Na^+ , K^+ -ATPase ($p = 0.667$) or ENaC ($p = 0.227$) was observed after treatment of A549 monolayers with OA (100 μ M) for 20 minutes (Figures 7A and 7B). Thus, OA does not inhibit

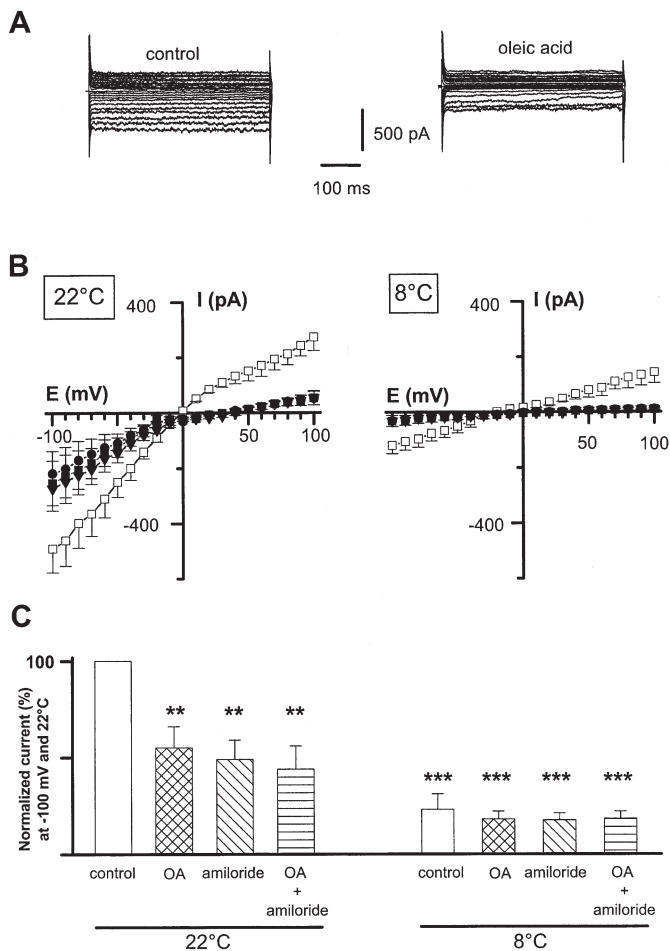


Figure 5. OA blocks whole-cell sodium currents in A549 cells. (A) Representative 500-millisecond traces demonstrate whole-cell currents in control and after 5-minute exposure to OA (10 μ M). Currents were evoked by applying incremental depolarizing 10-mV voltage steps between -100 and $+100$ mV every 10 seconds from a holding potential of -40 mV. (B) Averaged whole-cell current-voltage plots of total (open squares), OA-sensitive (solid circles), amiloride-sensitive (solid squares), and OA- and amiloride-sensitive (inverted solid triangles) steady-state currents at 22°C (left) and at 8°C (right). Values represent the mean \pm SD ($n = 6$ for each group). The OA-sensitive currents were obtained by subtracting residual current in B from total current in A. (C) Summarized data of normalized current elicited by a test potential at -100 mV in the control, after perfusion with OA (10 μ M), amiloride (10 μ M), or OA (10 μ M) plus amiloride (10 μ M; $n = 6$ for each group). ** $p < 0.01$; *** $p < 0.001$ in comparison to the control at 22°C .

transepithelial sodium transport by reducing cell-surface expression of Na^+, K^+ -ATPase or ENaC, either by preventing their exocytosis or promoting their endocytosis.

Immunoprecipitates of Na^+, K^+ -ATPase α subunit and ENaC β subunit were prepared from live cells incubated with (9,10[n]- ^3H)OA for 1 hour. After resolution by SDS-PAGE, bands at positions corresponding to the molecular masses of Na^+, K^+ -ATPase α subunit and ENaC β subunit were evident after autoradiography. Thus, OA associates, most likely covalently, with both molecules (Figure 7C).

Oleic Acid Directly Inhibits the ATPase Activity of the Na^+, K^+ -ATPase

OA potently, dose-dependently, and directly inhibited the ouabain-sensitive ATP-hydrolyzing activity of the catalytic α subunit

of the Na^+, K^+ -ATPase (Figure 8). At 100 μM OA, ouabain-sensitive ATP hydrolysis by Na^+, K^+ -ATPase was inhibited by a remarkable 98.6%. Significant ($p < 0.01$) inhibition of ATPase activity was attained over a concentration range of 20 to 100 μM OA. No effect on ATPase activity was observed in the presence of vehicle (0.17% [vol/vol] ethanol) alone.

DISCUSSION

Lipid metabolism, in particular free fatty acid dynamics, is an emerging area of interest in the pathogenesis of ARDS. OA, in particular, has been implicated in the pathogenesis of ARDS, and has been identified as a prognostic factor for this syndrome. OA levels are elevated in the circulation (16, 17) and in the alveolar fluids from patients with ARDS (21) and in the circulation of patients with sepsis that later develop ARDS (19). Furthermore, OA-induced lung injury is an extensively used experimental model of ARDS (23). The precise mechanisms by which OA induces this lung edema have not been elucidated (23), although increases in pulmonary vascular permeability (24), resulting in extravascular lung water accumulation (25), have been proposed as one explanation. However, no study to date has investigated the effects that OA may have on active transepithelial sodium transport, which is a key process in the resolution of pulmonary edema.

The present study addressed this issue in an isolated, ventilated, and perfused rabbit lung model (29). The administration of OA (25 μM) to the vascular compartment had no appreciable effect on epithelial permeability as assessed by [^3H]mannitol (a small solute) and, in some cases, FITC-albumin (a large solute) transit. Clearly, one limitation of this model is that it is a blood- and protein-free system. Thus, for example, the contribution of the oncotic gradients established by the protein component of the blood is not accounted for. Furthermore, in *in vivo* models of OA-induced lung injury, an increase in the epithelial permeability to large solutes, such as albumin, has been reported (23, 42, 43). These studies have used considerably higher doses of OA than the doses we used here. In one such study (43), an intravenous bolus of 0.09 ml OA/kg was used, yielding plasma concentrations of approximately 5 mM. Even if 95% of this OA associated with plasma proteins, the remaining 5%, which translates to a plasma concentration of approximately 200 μM , would be sufficient to cause changes in epithelial permeability. Furthermore, when we applied 200 μM OA in our isolated, ventilated, and perfused rabbit lung model, a 4.8-fold increase in epithelial permeability to large solutes, as assessed by FITC-albumin transit, was observed, with a concomitant marked increase in ELF volume and lung weight gain (results not shown). Therefore, OA (25 μM) was routinely used in the isolated, ventilated, and perfused rabbit lungs throughout this study.

Although epithelial permeability was unaffected, the endothelial permeability was increased up to 1.8-fold by the end of the experiment, when 25 μM OA was used. These data are consistent with reports that *Escherichia coli* endotoxin (44) and *Clostridium botulinum* C2 toxin (45) increase the endothelial permeability without any apparent effect on the epithelial permeability. In contrast, the administration of OA to the vascular compartment of the lung dramatically reduced the active transepithelial sodium transport by 92%. This observation paralleled the effect of low temperature, where all active transport processes are blocked. The sodium channel inhibitor amiloride caused a partial (58%) block of active transepithelial sodium transport. This result is consistent with reports that approximately 50% of the sodium transport channels in mammalian lungs are amiloride-sensitive (10, 40). These observations led us to believe that, in addition to amiloride-sensitive sodium channels,

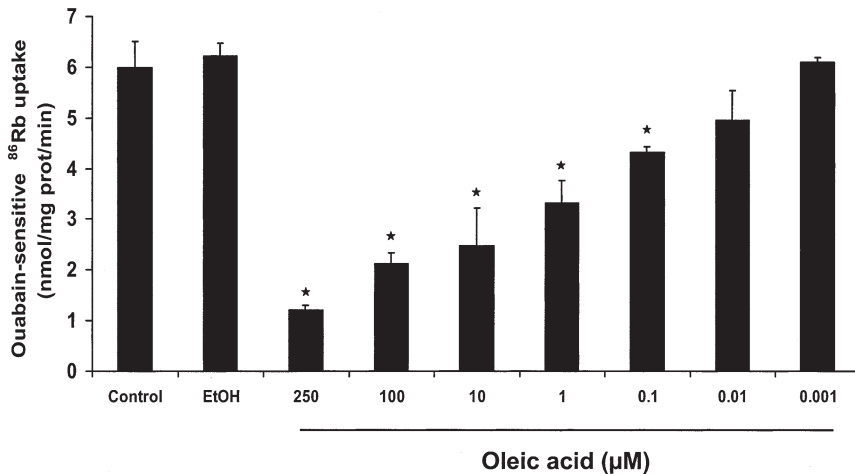


Figure 6. OA blocks ouabain-sensitive ⁸⁶Rb⁺ uptake by A549 cells in a dose-dependant manner. The uptake of ⁸⁶Rb⁺ by A549 cells was assessed in the presence of various concentrations of OA (1 nM–250 µM), or in the presence of vehicle alone (0.17% [vol/vol] ethanol [EtOH] in the media). Each bar represents the mean ± SD (n = 6 for each condition); *p < 0.001. Prot = protein.

OA inhibited other active sodium transport processes in the lung. To further explore this phenomenon, we investigated the effect of OA on sodium channel activity and sodium pump activity of epithelial cells *in vitro*.

When whole-cell current of lung epithelial cells was measured by patch clamp, OA blocked sodium current by 55 ± 11%. The application of OA with amiloride either at 22 or at 8°C did not significantly increase the degree to which sodium current was blocked, compared with that observed when amiloride was applied alone. Low temperature resulted in a fourfold decrease (down to 23 ± 8%) in whole-cell current, compared with whole-cell current at 22°C at –100 mV. Although some literature suggests that the activity of ENaC-type channels is increased at low temperature (46, 47), subsequent studies have shown that the single-channel conductance of ENaC decreased by 50% when the temperature of the perfusion solution was lowered from 30 to 15°C (48). Our data are consistent with these observations, and with those of other investigators who observed a similar phenomenon with cyclic GMP-gated channels (49). Together, these data indicated that OA inhibited the amiloride-sensitive channels in A549 cells. Because the active sodium transport block that we observed in intact lungs surpassed that observed with amiloride, we suspected that other active sodium transport processes in the lung were also affected by OA.

We therefore shifted our focus to the Na⁺,K⁺-ATPase, which plays a pivotal role in the active transport of sodium from alveolar epithelial cells into the interstitium. This is an essential step in generating the osmotic gradient that clears fluid from the alveolar space. The importance of the Na⁺,K⁺-ATPase in the resolution of edema has been underscored by the observation that adenoviral-mediated transfer of an Na⁺,K⁺-ATPase subunit gene to the alveolar epithelium promoted the resolution of acute hydrostatic pulmonary edema (50) and pulmonary edema elicited by hyperoxic (51) and ventilator-induced lung injury (52). Furthermore, OA dose-dependently impaired the Na⁺,K⁺-ATPase-mediated uptake of ⁸⁶Rb⁺ by lung epithelial cells.

Together, our data from the intact lungs and cell culture studies indicate that OA impairs not only one, but both of the essential mechanisms of transepithelial active sodium transport in the lung. OA inhibits active transport of sodium from the alveolar space into the alveolar epithelial cells, mediated by amiloride-sensitive sodium channels, and also inhibits the subsequent extrusion of sodium from the alveolar epithelial cell into the interstitium, mediated by Na⁺,K⁺-ATPase. In this way, OA dramatically blocks any capacity of the lung to clear edema fluid.

We also demonstrated in this study that OA causes an increase in the endothelial permeability of isolated, ventilated, and perfused rabbit lungs, which has also been observed by other investigators after intravenous administration of OA to dogs (24). Thus, OA both *promotes* alveolar and/or interstitial flooding by increasing the endothelial permeability and *prevents* fluid clearance by blocking active sodium transport.

This “dual effect” of OA on lung fluid homeostasis was also reflected by the increase in lung weight gain. In our protocol, approximately 2 ml of fluid was nebulized into the alveolar spaces of the ventilated lungs. The weight gain we observed was exclusively caused by the fluid that is nebulized into the lungs. Healthy lungs can effectively clear this fluid because their sodium transport processes are intact and functional. Lungs treated with low temperature (which blocks active processes) or with agents, such as amiloride and OA (which block active sodium transport), cannot clear this excess fluid. Control lungs maintained at 37°C over the course of the experiment exhibited transient weight gains after each nebulization (of ~ 1 g, corresponding to 1 ml of fluid nebulized into the lung per nebulization), but a net weight loss of 0.12 g by the end of the experiment (thus, in total, 2.12 g of fluid was cleared from the lungs; Figure 3A). In lungs maintained at 4°C, a net weight gain of 1.5 g and a 2-ml increase in ELF volume were observed at the conclusion of the experiment, representing fluid that could not be cleared out of the lungs because the active fluid clearance processes were blocked at 4°C. A parallel situation was also observed when amiloride, a selective sodium channel blocker, and OA were applied. In both instances, active transport processes were blocked, and fluid could not be cleared out of the lungs. This effect was less dramatic in the case of amiloride, because only approximately 60% of the sodium transport channels in the alveolar epithelium are amiloride-sensitive (40). Similarly, application of OA and amiloride together and separately at 4°C did not have any additive effect. Thus, low temperature, amiloride, and OA must be targeting the same process: active transepithelial sodium transport. We concluded that the weight gains and ELF volume increases that we observed were a direct consequence of blocked active sodium clearance.

Under the experimental conditions, the increase in ELF volume is greater than the apparent net weight gain of the lung. This finding is probably because of a vasoconstriction of the lung that developed under conditions of low temperature and OA administration. This mild vasoconstriction causes a small reduction in the vascular space, and thereby a decrease in the

lungs by blocking active sodium transport. We have further demonstrated that OA directly interacts with, and thus suppresses, both amiloride-sensitive sodium channels and the Na^+/K^+ -ATPase pump. However, we believe that our data extend beyond the simple explanation of an OA-induced lung injury model because they have several clinical implications. Lipid emulsions containing 1 to 2% OA are administered intravenously for parenteral nutrition in patients with sepsis, although their impact on clinical outcome is not clear (19). Furthermore, OA has been implicated both in the pathogenesis of ARDS and as a prognostic factor for ARDS. OA levels are elevated in the circulation (16, 17) and in the alveolar fluids of patients with ARDS (21), and in the circulation of patients with sepsis who later develop ARDS (19). Elevated OA levels are also provoked in the BAL fluids in an LPS-induced ARDS model (20). Thus, we propose that OA represents more than simply an ARDS model or a prognostic factor for this syndrome, but rather, that OA itself may be a mediator of ARDS.

Conflict of Interest Statement: I.V. does not have a financial relationship with a commercial entity that has an interest in the subject of this manuscript; R.E.M. does not have a financial relationship with a commercial entity that has an interest in the subject of this manuscript; M.G.K. does not have a financial relationship with a commercial entity that has an interest in the subject of this manuscript; A.O. does not have a financial relationship with a commercial entity that has an interest in the subject of this manuscript; F.G. receives grant and contract support from Pfizer Ltd. and Altana Pharma AG and serves on the advisory board of Altana Pharma AG; W.S. receives grant and contract support from Schering AG, Pfizer Ltd., Altana Pharma AG, Lung Rx, and Myogen; H.A.G. receives grant and contract support from Pfizer Ltd. and serves on advisory boards of Pfizer, Schering, and Altana Pharma.

Acknowledgment: The authors thank Professor Jacob I. Sznajder (Northwestern University School of Medicine, Chicago, IL) for expert advice and critical reading of the manuscript, and Bastian Eul and Sebastian Rummel for their outstanding support.

References

- Ware LB, Matthay MA. The acute respiratory distress syndrome. *N Engl J Med* 2000;342:1334–1349.
- Zilberberg MD, Epstein SK. Acute lung injury in the medical ICU: comorbid conditions, age, etiology, and hospital outcome. *Am J Respir Crit Care Med* 1998;157:1159–1164.
- Network ARDS. Ventilation with lower tidal volumes as compared with traditional tidal volumes for acute lung injury and the acute respiratory distress syndrome. The Acute Respiratory Distress Syndrome Network. *N Engl J Med* 2000;342:1301–1308.
- Kollef MH, Schuster DP. The acute respiratory distress syndrome. *N Engl J Med* 1995;332:27–37.
- Matthay MA, Wiener-Kronish JP. Intact epithelial barrier function is critical for the resolution of alveolar edema in humans. *Am Rev Respir Dis* 1990;142:1250–1257.
- Sznajder JI. Strategies to increase alveolar epithelial fluid removal in the injured lung. *Am J Respir Crit Care Med* 1999;160:1441–1442.
- Matthay MA. Alveolar fluid clearance in patients with ARDS: does it make a difference? *Chest* 2002;122:340S–343S.
- Sznajder JI. Alveolar edema must be cleared for the acute respiratory distress syndrome patient to survive. *Am J Respir Crit Care Med* 2001;163:1293–1294.
- Matthay MA, Clerici C, Saumon G. Invited review: active fluid clearance from the distal air spaces of the lung. *J Appl Physiol* 2002;93:1533–1541.
- Matthay MA, Folkesson HG, Clerici C. Lung epithelial fluid transport and the resolution of pulmonary edema. *Physiol Rev* 2002;82:569–600.
- Kellenberger S, Schild L. Epithelial sodium channel/degenerin family of ion channels: a variety of functions for a shared structure. *Physiol Rev* 2002;82:735–767.
- Matalon S, O'Brodoovich H. Sodium channels in alveolar epithelial cells: molecular characterization, biophysical properties, and physiological significance. *Annu Rev Physiol* 1999;61:627–661.
- Skou JC, Esmann M. The Na^+/K^+ -ATPase. *J Bioenerg Biomembr* 1992;24:249–261.
- Factor P, Saldias F, Ridge K, Dumasius V, Zabner J, Jaffe HA, Blanco G, Barnard M, Mercer R, Perrin R, et al. Augmentation of lung liquid clearance via adenovirus-mediated transfer of a Na^+/K^+ -ATPase beta1 subunit gene. *J Clin Invest* 1998;102:1421–1430.
- Sznajder JI, Factor P, Ingbar DH. Invited review: lung edema clearance: role of Na^+/K^+ -ATPase. *J Appl Physiol* 2002;93:1860–1866.
- Quinlan GJ, Lamb NJ, Evans TW, Gutteridge JM. Plasma fatty acid changes and increased lipid peroxidation in patients with adult respiratory distress syndrome. *Crit Care Med* 1996;24:241–246.
- Bursten SL, Federighi DA, Parsons P, Harris WE, Abraham E, Moore EE Jr, Moore FA, Bianco JA, Singer JW, Repine JE. An increase in serum C18 unsaturated free fatty acids as a predictor of the development of acute respiratory distress syndrome. *Crit Care Med* 1996;24:1129–1136.
- Hudson LD, Milberg JA, Anardi D, Maunder RJ. Clinical risks for development of the acute respiratory distress syndrome. *Am J Respir Crit Care Med* 1995;151:293–301.
- Mayer K, Gokorsch S, Fegbeutel C, Hattar K, Rosseau S, Walrath D, Seeger W, Grimminger F. Parenteral nutrition with fish oil modulates cytokine response in patients with sepsis. *Am J Respir Crit Care Med* 2003;167:1321–1328.
- Arbibe L, Koumanov K, Vial D, Rougeot C, Faure G, Havet N, Longacre S, Vargaftig BB, Bereziat G, Voelker DR, et al. Generation of lysophospholipids from surfactant in acute lung injury is mediated by type-II phospholipase A2 and inhibited by a direct surfactant protein A-phospholipase A2 protein interaction. *J Clin Invest* 1998;102:1152–1160.
- Schmidt R, Meier U, Yabut-Perez M, Walrath D, Grimminger F, Seeger W, Gunther A. Alteration of fatty acid profiles in different pulmonary surfactant phospholipids in acute respiratory distress syndrome and severe pneumonia. *Am J Respir Crit Care Med* 2001;163:95–100.
- Gunther A, Schmidt R, Harodt J, Schmehl T, Walrath D, Ruppert C, Grimminger F, Seeger W. Bronchoscopic administration of bovine natural surfactant in ARDS and septic shock: impact on biophysical and biochemical surfactant properties. *Eur Respir J* 2002;19:797–804.
- Schuster DP. ARDS: clinical lessons from the oleic acid model of acute lung injury. *Am J Respir Crit Care Med* 1994;149:245–260.
- Motohiro A, Furukawa T, Yasumoto K, Inokuchi K. Mechanisms involved in acute lung edema induced in dogs by oleic acid. *Eur Surg Res* 1986;18:50–57.
- Ashbaugh DG, Uzawa T. Respiratory and hemodynamic changes after injection of free fatty acids. *J Surg Res* 1968;8:417–423.
- Vadász I, Ghofrani HA, Grimminger F, Seeger W, Kohstall MG. Effect of oleic acid on active and passive sodium clearance in an isolated, ventilated and perfused rabbit lung model [abstract]. *Am J Respir Crit Care Med* 2004;160:A708.
- Seeger W, Walrath D, Grimminger F, Rosseau S, Schutte H, Kramer HJ, Ermert L, Kiss L. Adult respiratory distress syndrome: model systems using isolated perfused rabbit lungs. *Methods Enzymol* 1994;233:549–584.
- Lecuona E, Saldias F, Comellas A, Ridge K, Guerrero C, Sznajder JI. Ventilator-associated lung injury decreases lung ability to clear edema in rats. *Am J Respir Crit Care Med* 1999;159:603–609.
- Ghofrani HA, Kohstall MG, Weissmann N, Schmehl T, Schemmly RT, Seeger W, Grimminger F. Alveolar epithelial barrier functions in ventilated perfused rabbit lungs. *Am J Physiol Lung Cell Mol Physiol* 2001;280:L896–L904.
- Schutte H, Hermle G, Seeger W, Grimminger F. Vascular distension and continued ventilation are protective in lung ischemia/reperfusion. *Am J Respir Crit Care Med* 1998;157:171–177.
- Seeger W, Walrath D, Menger M, Neuhof H. Increased lung vascular permeability after arachidonic acid and hydrostatic challenge. *J Appl Physiol* 1986;61:1781–1789.
- Hamill OP, Marty A, Neher E, Sakmann B, Sigworth FJ. Improved patch-clamp techniques for high-resolution current recording from cells and cell-free membrane patches. *Pflugers Arch* 1981;391:85–100.
- Lazrak A, Samanta A, Matalon S. Biophysical properties and molecular characterization of amiloride-sensitive sodium channels in A549 cells. *Am J Physiol Lung Cell Mol Physiol* 2000;278:L848–L857.
- Ridge KM, Dada L, Lecuona E, Bertorello AM, Katz AI, Mochly-Rosen D, Sznajder JI. Dopamine-induced exocytosis of Na^+/K^+ -ATPase is dependent on activation of protein kinase C-epsilon and -delta. *Mol Biol Cell* 2002;13:1381–1389.
- Bradford MM. A rapid and sensitive method for the quantitation of microgram quantities of protein utilizing the principle of protein-dye binding. *Anal Biochem* 1976;72:248–254.
- Schagger H, von Jagow G. Tricine-sodium dodecyl sulfate-polyacrylamide gel electrophoresis for the separation of proteins in the range from 1 to 100 kDa. *Anal Biochem* 1987;166:368–379.
- Dada LA, Chandel NS, Ridge KM, Pedemonte C, Bertorello AM, Sznajder JI. Hypoxia-induced endocytosis of Na^+/K^+ -ATPase in alveolar

- epithelial cells is mediated by mitochondrial reactive oxygen species and PKC-zeta. *J Clin Invest* 2003;111:1057–1064.
38. Holliday CW. Salinity-induced changes in gill Na, K-ATPase activity in the mud fiddler crab, *Uca pugnax*. *J Exp Zool* 1985;233:199–208.
 39. Rutschman DH, Olivera W, Sznajder JI. Active transport and passive liquid movement in isolated perfused rat lungs. *J Appl Physiol* 1993;75:1574–1580.
 40. Nielsen VG, Duvall MD, Baird MS, Matalon S. cAMP activation of chloride and fluid secretion across the rabbit alveolar epithelium. *Am J Physiol* 1998;275:L1127–L1133.
 41. Yue G, Matalon S. Mechanisms and sequelae of increased alveolar fluid clearance in hyperoxic rats. *Am J Physiol* 1997;272:L407–L412.
 42. Kato S, Asai T, Ono K, Onuma N, Nakamoto T, Iizuka M. Albumin and fibronectin dynamics in an experimental acute respiratory distress syndrome model. *Nihon Kyobu Shikkan Gakkai Zasshi* 1993;31:431–440.
 43. Su X, Bai C, Hong Q, Zhu D, He L, Wu J, Ding F, Fang X, Matthay MA. Effect of continuous hemofiltration on hemodynamics, lung inflammation and pulmonary edema in a canine model of acute lung injury. *Intensive Care Med* 2003;29:2034–2042.
 44. Wiener-Kronish JP, Albertine KH, Matthay MA. Differential responses of the endothelial and epithelial barriers of the lung in sheep to Escherichia coli endotoxin. *J Clin Invest* 1991;88:864–875.
 45. Ermert L, Rossig R, Hansen T, Schutte H, Aktories K, Seeger W. Differential role of actin in lung endothelial and epithelial barrier properties in perfused rabbit lungs. *Eur Respir J* 1996;9:93–99.
 46. Askwith CC, Benson CJ, Welsh MJ, Snyder PM. DEG/ENaC ion channels involved in sensory transduction and modulated by cold temperature. *Proc Natl Acad Sci U S A* 2001;98:6459–6463.
 47. Chraïbi A, Horisberger JD. Na self inhibition of human epithelial Na channel: temperature dependence and effect of extracellular proteases. *J Gen Physiol* 2002;120:133–145.
 48. Chraïbi A, Horisberger JD. Dual effect of temperature on the human epithelial Na⁺ channel. *Pflugers Arch* 2003;447:316–320.
 49. Sesti F, Nizzari M, Torre V. Effect of changing temperature on the ionic permeation through the cyclic GMP-gated channel from vertebrate photoreceptors. *Biophys J* 1996;70:2616–2639.
 50. Azzam ZS, Dumasius V, Saldias FJ, Adir Y, Sznajder JI, Factor P. Na,K-ATPase overexpression improves alveolar fluid clearance in a rat model of elevated left atrial pressure. *Circulation* 2002;105:497–501.
 51. Factor P, Dumasius V, Saldias F, Brown LA, Sznajder JI. Adenovirus-mediated transfer of an Na⁺/K⁺-ATPase beta1 subunit gene improves alveolar fluid clearance and survival in hyperoxic rats. *Hum Gene Ther* 2000;11:2231–2242.
 52. Adir Y, Factor P, Dumasius V, Ridge KM, Sznajder JI. Na,K-ATPase gene transfer increases liquid clearance during ventilation-induced lung injury. *Am J Respir Crit Care Med* 2003;168:1445–1448.
 53. Shimkets RA, Lifton RP, Canessa CM. The activity of the epithelial sodium channel is regulated by clathrin-mediated endocytosis. *J Biol Chem* 1997;272:25537–25541.
 54. Xiao YF, Wright SN, Wang GK, Morgan JP, Leaf A. Fatty acids suppress voltage-gated Na⁺ currents in HEK293t cells transfected with the alpha-subunit of the human cardiac Na⁺ channel. *Proc Natl Acad Sci U S A* 1998;95:2680–2685.
 55. Swarts HG, Schuurmans Stekhoven FM, De Pont JJ. Binding of unsaturated fatty acids to Na⁺, K(+) -ATPase leading to inhibition and inactivation. *Biochim Biophys Acta* 1990;1024:32–40.
 56. Lu G, Greene EL, Nagai T, Egan BM. Reactive oxygen species are critical in the oleic acid-mediated mitogenic signaling pathway in vascular smooth muscle cells. *Hypertension* 1998;32:1003–1010.
 57. Matalon S, Hardiman KM, Jain L, Eaton DC, Kotlikoff M, Eu JP, Sun J, Meissner G, Stamler JS. Regulation of ion channel structure and function by reactive oxygen-nitrogen species. *Am J Physiol Lung Cell Mol Physiol* 2003;285:L1184–L1189.
 58. Bauer ML, Beckman JS, Bridges RJ, Fuller CM, Matalon S. Peroxynitrite inhibits sodium uptake in rat colonic membrane vesicles. *Biochim Biophys Acta* 1992;1104:87–94.
 59. Hu P, Ischiropoulos H, Beckman JS, Matalon S. Peroxynitrite inhibition of oxygen consumption and sodium transport in alveolar type II cells. *Am J Physiol* 1994;266:L628–L634.
 60. Jain L, Chen XJ, Brown LA, Eaton DC. Nitric oxide inhibits lung sodium transport through a cGMP-mediated inhibition of epithelial cation channels. *Am J Physiol* 1998;274:L475–L484.
 61. Chen L, Fuller CM, Kleyman TR, Matalon S. Mutations in the extracellular loop of alpha-rENaC alter sensitivity to amiloride and reactive species. *Am J Physiol Renal Physiol* 2004;286:F1202–F1208.
 62. Heberlein W, Wodopia R, Bartsch P, Mairbaur H. Possible role of ROS as mediators of hypoxia-induced ion transport inhibition of alveolar epithelial cells. *Am J Physiol Lung Cell Mol Physiol* 2000;278:L640–L648.
 63. Hamilton JA. Medium-chain fatty acid binding to albumin and transfer to phospholipid bilayers. *Proc Natl Acad Sci U S A* 1989;86:2663–2667.
 64. Clarke AL, Petrou S, Walsh JV Jr, Singer JJ. Modulation of BK(Ca) channel activity by fatty acids: structural requirements and mechanism of action. *Am J Physiol Cell Physiol* 2002;283:C1441–C1453.